J|A|C|S
ARTICLES
Published on Web 00/00/0000

Inhibitor Scaffolds as New Allele Specific Kinase Substrates

Brian C. Kraybill,[†] Lisa L. Elkin,[‡] Justin D. Blethrow,[†] David O. Morgan,[§] and Kevan M. Shokat*[,†,⊥]

Contribution from the Department of Cellular and Molecular Pharmacology, Box 0450, University of California— San Francisco, San Francisco, California 94143, Cellular Genomics Inc., 36 East Industrial Road, Branford, Connecticut 06405, the Department of Physiology and Biochemistry and Biophysics, Box 0444, University of California—San Francisco, San Francisco, California 94143, and the Department of Chemistry, University of California—Berkeley, Berkeley, California 94720

Received April 9, 2002. Revised Manuscript Received July 17, 2002

Abstract: The elucidation of protein kinase signaling networks is challenging due to the large size of the protein kinase superfamily (>500 human kinases). Here we describe a new class of orthogonal triphosphate substrate analogues for the direct labeling of analogue-specific kinase protein targets. These analogues were constructed as derivatives of the Src family kinase inhibitor PP1 and were designed based on the crystal structures of PP1 bound to HCK and N^6-(benzyl)-ADP bound to c-Src (T338G). 3-Benzylpyrazolopyrimidine triphosphate (3-benzyl-PPTP) proved to be a substrate for a mutant of the MAP kinase p38 (p38-T106G/A157L/L167A). 3-Benzyl-PPTP was preferred by v-Src (T338G) ($k_{cat}/K_M = 3.2 \times 10^6$ min^{-1} M^{-1}) over ATP or the previously described ATP analogue, N^6 (benzyl) ATP. For the kinase CDK2 (F80G)/cyclin E, 3-benzyl-PPTP demonstrated catalytic efficiency ($k_{cat}/K_M = 2.6 \times 10^4$ min^{-1} M^{-1}) comparable to ATP ($k_{cat}/K_M = 5.0 \times 10^4$ min^{-1} M^{-1}) largely due to a significantly better K_M (6.4 μM vs 530 μM). In kinase protein substrate labeling experiments both 3-benzyl-PPTP and 3-phenyl-PPTP prove to be over 4 times more orthogonal than N^6-(benzyl)-ATP with respect to the wild-type kinases found in murine spleenocyte cell lysates. These experiments also demonstrate that [γ-^{32}P]-3-benzyl-PPTP is an excellent phosphodonor for labeling the direct protein substrates of CDK2 (F80G)/E in murine spleenocyte cell lysates, even while competing with cellular levels (4 mM) of unlabeled ATP. The fact that this new more highly orthogonal nucleotide is accepted by three widely divergent kinases studied here suggests that it is likely to be generalizable across the entire kinase superfamily.

Introduction

Protein kinases are the central components of information transfer in cells.[1] They comprise the largest superfamily of signaling proteins in all organisms from plants to humans. One challenge in the post-genomic era is to identify the direct substrates of each protein kinase in the genome. This information would provide the necessary road map for understanding complex phenomena in cell signaling such as cross-talk between kinase pathways, signal amplification, desensitization to stimulation, molecular memory, and others.[2] We and others have developed multiple strategies for kinase substrate identification including chemical genetics,[3] protein chip technology,[4] combinatorial peptide screening,[5] phage display screening,[6] modulation of divalent metal requirements,[7] and use of highly specific kinase inhibitors to transiently inhibit targets.[8] The central problem each method attempts to overcome is that all kinases accept ATP as the phosphodonor substrate. Therefore, the activity of the kinase of interest must be isolatable either spatially (i.e., protein chips) or by use of highly selective small molecules capable of reporting on the activity of a single kinase in the cell.

Our laboratory has focused on the development of orthogonal ATP analogues, which can be used by mutant protein kinases.[9−11] A single, highly conserved amino acid in the ATP binding pocket of all kinases is mutated to glycine in order to create a new pocket capable of accepting [γ-^{32}P]-N^6-(benzyl)-ATP as a

* To whom correspondence should be addressed. E-mail: shokat@cmp.ucsf.edu.
† Department of Cellular and Molecular Pharmacology, University of California—San Francisco.
‡ Cellular Genomics Inc.
§ Department of Physiology and Biochemistry and Biophysics, University of California—San Francisco.
⊥ Department of Chemistry, University of California—Berkeley.

(1) Hunter, T. *Cell* **1995**, *80*, 225−36.
(2) Hunter, T. *Cell* **2000**, *100*, 113−27.
(3) Shah, K.; Shokat, K. M. *Chem. Biol.* **2002**, *9*, 35−47.
(4) Zhu, H.; Klemic, J. F.; Chang, S.; Bertone, P.; Casamayor, A.; Klemic, K. G.; Smith, D.; Gerstein, M.; Reed, M. A.; Snyder, M. *Nat. Genet.* **2000**, *26*, 283−9.
(5) Songyang, Z.; Blechner, S.; Hoagland, N.; Hoekstra, M. F.; Piwnica-Worms, H.; Cantley, L. C. *Curr. Biol.* **1994**, *4*, 973−982.
(6) Fukunaga, R.; Hunter, T. *EMBO J.* **1997**, *16*, 1921−33.
(7) Knebel, A.; Morrice, N.; Cohen, P. *EMBO J.* **2001**, *20*, 4360−9.
(8) Holmstrom, T. H.; Tran, S. E.; Johnson, V. L.; Ahn, N. G.; Chow, S. C.; Eriksson, J. E. *Mol. Cell. Biol.* **1999**, *19*, 5991−6002.
(9) Liu, Y.; Shah, K.; Yang, F.; Witucki, L.; Shokat, K. M. *Bioorg. Med. Chem.* **1998**, *6*, 1219−26.
(10) Liu, Y.; Shah, K.; Yang, F.; Witucki, L.; Shokat, K. M. *Chem. Biol.* **1998**, *5*, 91−101.
(11) Shah, K.; Liu, Y.; Deirmengian, C.; Shokat, K. M. *Proc. Natl. Acad. Sci. U. S. A.* **1997**, *94*, 3565−70.

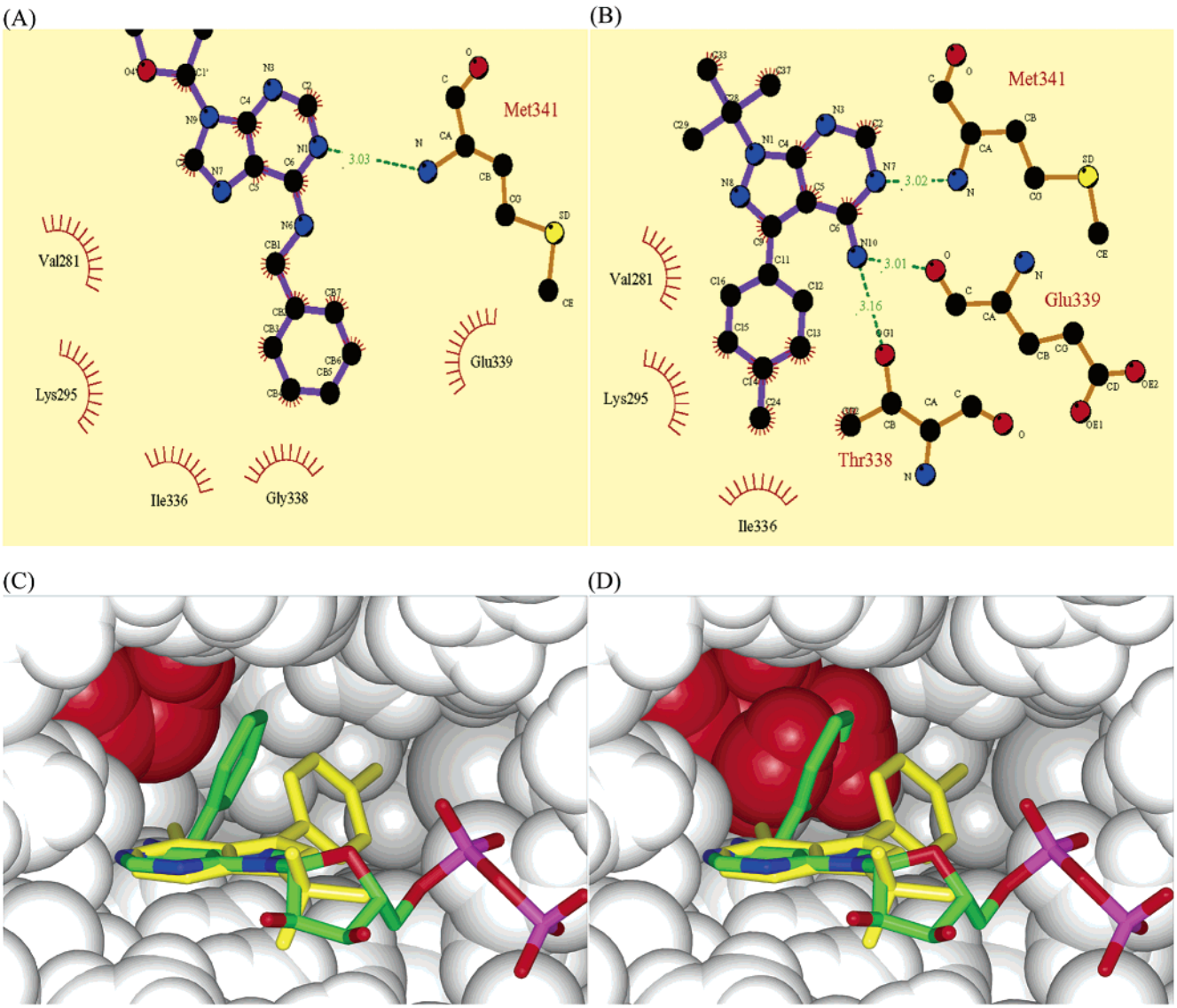

Figure 1. Ligplot and Insight II representations of the Src family kinase Hck bound to PP1 (PBD ID: 1KSW) and c-Src-as1 bound to N^6-(benzyl)-ADP (1QCF) crystal structures. PP1 is colored yellow, while N^6-(benzyl)-ADP is colored by atom type (C = green, N = blue, O = red, P = purple). (A) Ligplot of N^6-(benzyl)-ADP bound to c-Src-as1. (B) Ligplot of PP1 bound to Hck. (C) Insight II view of N^6-(benzyl)-ADP bound to c-Src-as1 (G338 in red) overlaid with PP1, where the steric clash is removed by the mutation and space for the benzyl group has been made. (D) Insight II view of N^6-(benzyl)-ADP overlaid with PP1 bound to Hck showing the steric clash between T338 (in red again) and the benzyl group of N^6-(benzyl)-ADP. The Insight II views were made by aligning the backbones of the crystal structures of Hck bound to PP1 and the c-Src-as1 bound to N^6-(benzyl)-ADP. Residues covering the view of the pocket, including V281 and K295, have been removed to enhance viewing of the difference introduced by the mutation.

substrate. This ATP analogue is a poor substrate for wild-type protein kinases, making it a highly specific reagent for radiolabeling the direct substrates of the kinase of interest. This approach has been used to identify cofilin and calumenin as novel targets of the oncogenic kinase v-Src,[3] hnRNP-K as a direct target of the stress-activated ser/thr kinase JNK,[12] and the karposi's sarcoma protein K-bZIP by cyclin-dependent kinase 2.[13]

In this study we set out to design a new ATP analogue with enhanced selectivity for mutant kinases. Our goal was to incorporate improved catalytic efficiency toward the mutants as well as orthogonality with respect to wild-type protein kinases. This is necessary in order to ultimately achieve the labeling of direct substrates in intact cells where competing kinases are highly active and competing nucleotide pools are large (4 mM).[14] Through structural analysis of the N^6-(benzyl)-ADP bound to c-Src-as1 (as = analogue specific, resulting from the T338G mutation) kinase[15] we have determined that the benzyl moiety at N^6 does indeed occupy the engineered pocket (Figure 1A,C). We also noticed that a large, naturally existing, hydrophobic pocket immediately adjacent to the benzyl moiety was not occupied by N^6-(benzyl)-ADP. We reasoned that by designing a new analogue capable of exploiting this naturally existing pocket, as well as the newly engineered pocket (T338G in c-Src), we could produce a more highly specific orthogonal ATP analogue for identification of direct kinase substrates.

(12) Habelhah, H.; Shah, K.; Huang, L.; Burlingame, A. L.; Shokat, K. M.; Ronai, Z. *J. Biol. Chem.* **2001**, *276*, 18090−5.
(13) Polson, A. G.; Huang, L.; Lukac, D. M.; Blethrow, J. D.; Morgan, D. O.; Burlingame, A. L.; Ganem, D. *J. Virol.* **2001**, *75*, 3175−84.
(14) Garby, L.; Larsen, P. S. *Bioenergetics: it's thermodynamic foundations*; Cambridge University Press: New York, 1995.
(15) Witucki, L. A.; Huang, X.; Shah, K.; Liu, Y.; Kyin, S.; Eck, M. J.; Shokat, K. M. *Chem. Biol.* **2002**, *9*, 25−33.

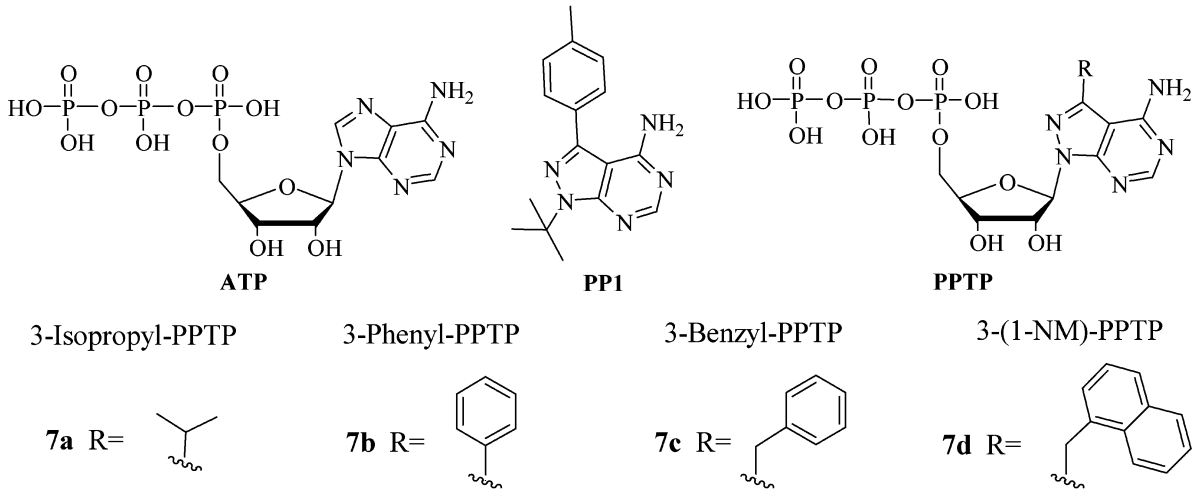

Figure 2. Structures of ATP, PP1, and PPTP (pyrazolopyrimidine triphosphate) analogues.

The unfilled pocket in the N^6-(benzyl)-ADP/c-Src-as1 kinase cocrystal structure is lined by Val 281, Lys 295, Ile 336, and Gly 338 (mutated from Thr to accommodate the benzyl substituent). To design a new scaffold for appropriate presentation of a substituent into this pocket we turned to several kinase inhibitor structures. Many kinase inhibitor scaffolds achieve potent and selective binding to particular kinases by presentation of substituents into this same pocket.[16] In particular, the Src-family-selective inhibitor PP1 contains a *p*-methylphenyl substituent that makes extensive contacts with each of the residues lining this pocket (Figure 1B,D).[17] In fact, our lab has recently identified derivatives of PP1 that are potent and highly selective inhibitors of many analogue sensitive mutant protein kinases.[18−20] These observations prompted us to take the unusual approach of redesigning the inhibitor PP1 to become a phosphodonor substrate for this enzyme. This is challenging because the requirements for substrate recognition and transition state stabilization are considerably different than those required of inhibitor binding to the same enzyme active site.[21]

Results and Discussion

Allele Specific Inhibitors Provide Potential Substrate Leads. The orientation of PP1 bound to the active site of the Src family kinase Hck[22]provides a conceptually simple approach for conversion of this potent inhibitor into a phosphodonor substrate. The pyrazolopyrimidine ring of PP1 is bound in the same orientation as the purine ring of ATP, fulfilling the stringent substrate recognition requirements in the purine binding pocket of the kinase. The *tert*-butyl substituent at N^1 of PP1 occupies the sugar binding pocket of Hck, as shown in the overlay of PP1 and N^6-(benzyl)-ADP in the Hck and c-Src-as1 crystal structures (Figure 1C,D). Replacement of the *tert*-butyl moiety of PP1 with a β-furanose-5′-triphosphate should produce a pyrazolopyrimidine triphosphate (PPTP) analogue suitable for a kinase to recognize as a substrate (Figure 2).

A key challenge in converting an inhibitor into a substrate stems from the fact that good inhibitors bind (K_D = 1−10 nM)[23,24] much more tightly than ATP (K_M = 5−600 μM)[25−29] to kinases. Unlike our previous inhibitor design efforts, we searched for substituents that would trade affinity for catalytic turnover. In addition, good allele-specific substrates must bind in a catalytically competent orientation. We synthesized a series of PPTP analogues with C^3 substituents designed to provide differential complementarity for the engineered active site in analogue specific kinases. Our goals were to identify a PPTP analogue with catalytic efficiency (k_{cat}/K_M) greater than that of the natural substrate ATP and the analogue N^6-(benzyl)-ATP for several analogue-specific kinase mutants and enhanced orthogonality with respect to all wild-type protein kinases.

The different substituents at the C^3 position were designed to probe the important determinants for inhibition versus efficient substrate utilization. Based on structure activity relationships with the PP1 inhibitor series we expected substituents larger than a phenyl ring would not likely be accepted by wild-type kinases (Figure 1D).[17] Mutation of the c-Src Thr 338 to Gly should enlarge the active site pocket and allow pyrazolopyrimidine triphosphate (PPTP) analogues to be accepted (Figure 1C).

Synthesis of PPTP Analogues. We chose to synthesize 3-isopropyl-PPTP (**7a**), 3-phenyl-PPTP (**7b**), 3-benzyl-PPTP (**7c**), and 3-(1-naphthylmethyl)-PPTP (**7d**) (Figure 2). Construction of the pyrazolopyrimidine heterocycle followed the original PP1 synthesis by Hanefeld et al. (Figure 3).[30] The appropriate

(16) Bishop, A. C.; Buzko, O.; Shokat, K. M. *Trends Cell Biol.* **2001**, *11*, 167−72.
(17) Liu, Y.; Bishop, A.; Witucki, L.; Kraybill, B.; Shimizu, E.; Tsien, J.; Ubersax, J.; Blethrow, J.; Morgan, D. O.; Shokat, K. M. *Chem. Biol.* **1999**, *6*, 671−8.
(18) Bishop, A. C.; Kung, C.-Y.; Shah, K.; Witucki, L.; Shokat, K. M.; Liu, Y. *J. Am. Chem. Soc.* **1999**, *121*, 627−631.
(19) Bishop, A. C.; Ubersax, J. A.; Petsch, D. T.; Matheos, D. P.; Gray, N. S.; Blethrow, J.; Shimizu, E.; Tsien, J. Z.; Schultz, P. G.; Rose, M. D.; Wood, J. L.; Morgan, D. O.; Shokat, K. M. *Nature* **2000**, *407*, 395−401.
(20) Bishop, A. C.; Shah, K.; Liu, Y.; Witucki, L.; Kung, C.; Shokat, K. M. *Curr. Biol.* **1998**, *8*, 257−66.
(21) Lin, Q.; Jiang, F.; Schultz, P. G.; Gray, N. S. *J. Am. Chem. Soc.* **2001**, *123*, 11608−13.
(22) Schindler, T.; Sicheri, F.; Pico, A.; Gazit, A.; Levitzki, A.; Kuriyan, J. *Mol. Cell* **1999**, *3*, 639−48.
(23) Davies, S. P.; Reddy, H.; Caivano, M.; Cohen, P. *Biochem. J.* **2000**, *351*, 95−105.
(24) Bridges, A. J. *Chem. Rev.* **2001**, *101*, 2541−72.
(25) Enke, D. A.; Kaldis, P.; Solomon, M. J. *J. Biol. Chem.* **2000**, *275*, 33267−71.
(26) Sun, G.; Ramdas, L.; Wang, W.; Vinci, J.; McMurray, J.; Budde, R. J. *Arch. Biochem. Biophys.* **2002**, *397*, 11−7.
(27) Lew, J.; Coruh, N.; Tsigelny, I.; Garrod, S.; Taylor, S. S. *J. Biol. Chem.* **1997**, *272*, 1507−13.
(28) Parast, C. V.; Mroczkowski, B.; Pinko, C.; Misialek, S.; Khambatta, G.; Appelt, K. *Biochemistry* **1998,** *37*, 16788−801.
(29) Chen, G.; Porter, M. D.; Bristol, J. R.; Fitzgibbon, M. J.; Pazhanisamy, S. *Biochemistry* **2000**, *39*, 2079−87.

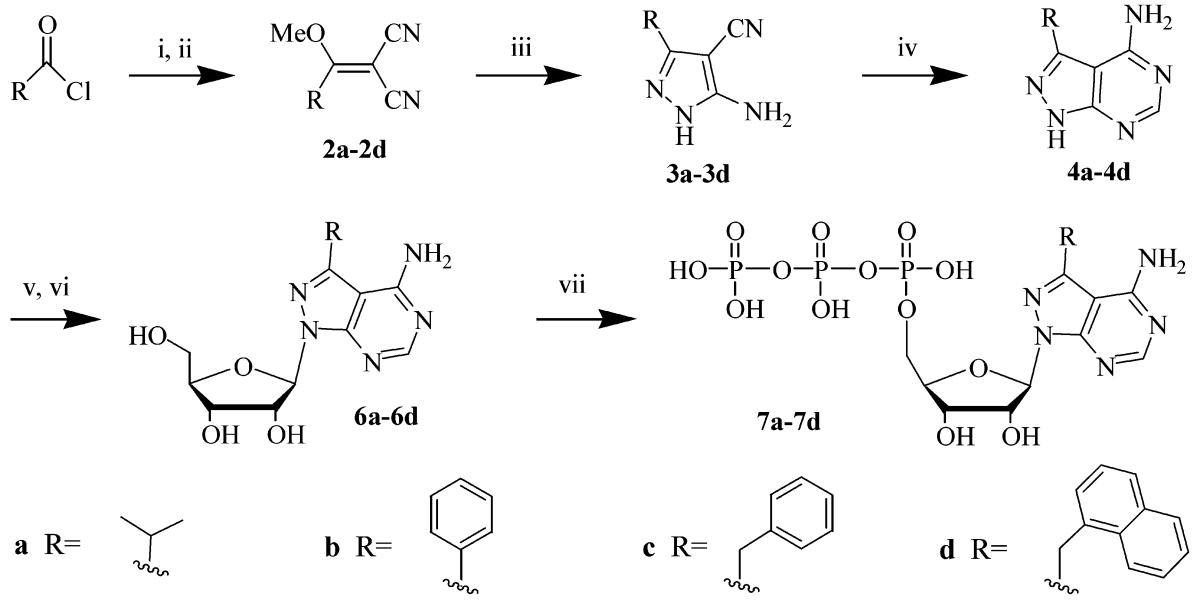

Figure 3. Synthesis of C^3-substituted PPTP analogues. Conditions: (i) 2 equiv of NaH, 1 equiv of malononitrile, THF, room temperature, 1 h, 81−95%; (ii) 8 equiv $NaHCO_3$, 7 equiv of dimethyl sulfate, dioxane/water (6/1), reflux, 2 h, 31−90%; (iii) 1 equiv of hydrazine dihydrochloride, 3 equiv of triethylamine, EtOH, reflux, 15 min, 52−84%; (iv) formamide, 180 °C, overnight, 60−72%; (v) 1 equiv of *β-d*-ribofuranose-1-acetate-2,3,5-tribenzoate, 2.5 equiv of $SnCl_4$, CH_3CN, room temperature, 5 h, 52−80%; (vi) 7 N NH_3 in MeOH, room temperature, 36 h, 64−83%; (vii) a) 3.2 equiv of $POCl_3$, PO_4Me_3, 0 °C, 40 min; b) 5 equiv of pyrophosphoric acid, 10 equiv of tributylamine, DMF, room temperature, 1 min, 1−5%.

R acid chloride was condensed with malononitrile using sodium hydride in THF. The product dicyanoenol (**1a**−**d**) was O-alkylated by using dimethyl sulfate with sodium bicarbonate in a 6:1 dioxane:water solution. This enol ether (**2a**−**d**) was condensed with hydrazine dihydrochloride in ethanol with triethylamine to produce the 5-amino-4-carbonitrilepyrazole (**3a**−**d**). The pyrimidine ring was formed (**4a**−**d**) by boiling in neat formamide. Alkylation of N^1 by the 2,3,5-tri-*O*-benzoyl-1-*O*-acetylribofuranose was effected by the lewis acid $SnCl_4$ in acetonitrile (**5a**−**d**).[31] The benzoyl protecting groups were removed with methanolic ammonia to yield the nucleosides (**6a**−**d**).

Triphosphate synthesis (**7a**−**d**) was accomplished following the general procedure of Ludwig et al.,[32] in which nucleoside was first reacted with phosphorus oxychloride in trimethyl phosphate. The 5′-phosphorus oxychloride adduct formed *in situ* was then treated with dry pyrophosphoric acid in 2 mL of DMF with 2 equiv of tributylamine, and the reaction was quenched with aqueous triethylammonium bicarbonate.

The synthesis of [γ-^{32}P]triphosphates utilized a chemoenzymatic approach.[13] Initially the diphosphate nucleotides were produced chemically by addition of phosphoric acid to the carbonyldiimidazole treated monophosphate nucleotides. Immobilized, recombinant, deca-histidine-tagged nucleoside diphosphate kinase (10X-His-NDPK) was then used to catalyze transfer of the γ-phosphate from [γ-^{32}P]ATP to the nucleotide diphosphate. The 10X-His-NDPK was immobilized on Co^{2+} IDA beads, autophosphorylated with [γ-^{32}P]ATP, and then washed extensively. Next the beads were treated with the analogue diphosphate. The NDPK catalyzed transfer of the [^{32}P]phosphate group from the phosphoryl histidine intermediate to the nucleotide diphosphate, producing the desired [γ-^{32}P]-labeled triphosphate analogue.

Identification of Catalytically Viable PPTP Substrates. The catalytic viability of our panel of PPTP analogues (**7a**−**d**) was first determined by using a bacterially expressed ser/thr kinase involved in the mitogenic signal transduction cascade. MAPK p38-wt and a mutant in which Thr 106 was mutated to glycine (p38-as3, also includes A157L and L167A) were expressed and purified in bacteria.[3333] Kinase reactions were conducted with PPTP analogues **7a**−**d** and the p38 protein substrate activating transcription factor 2 (ATF2). The ratio of phosphorylated ATF2 to total ATF2 was then determined by using antibodies specific for the phosphorylated or nonphosphorylated ATF2 forms in an ELISA assay.[34] The data are presented here as a comparison of the ratio of phospho/nonphospho specific antibody binding determined for each analogue compared with the ratio achieved with ATP (Figure 4). This analysis showed that the analogues **7b** and **7c** were indeed substrates for p38-as3 and not for p38-wt. Analogues **7a** and **7d** were not substrates for any p38 kinase alleles tested and so were not investigated further.

Since our goal was to discover a new ATP analogue that could be utilized by any suitably engineered kinase, we further tested **7b** and **7c** with a different protein kinase, distantly related to p38. Cyclin-dependent kinase 2/cyclin E (CDK2/E) is the critical S phase kinase involved in progression through this early phase of the mammalian cell cycle. Few bona fide direct substrates of CDK2/E are known, making the identification of its substrates critical for understanding the mammalian cell cycle.[35] The analogue-sensitive human CDK2-as1/E was tested for the ability to utilize **7b** and **7c**, the two best substrates for the map kinase p38-as3.

(30) Hanefeld, U.; Rees, C. W.; White, A. J. P.; Williams, D. J. *J. Chem. Soc., Perkin Trans. 1* **1996,** 1545−1552.
(31) Saneyoshi, M.; Satoh, E. *Chem. Pharm. Bull.* **1979**, *27*, 2518−2521.
(32) Ludwig, J. *J. Acta Biochim. Biophys.* **1981**, *16*, 131−133.
(33) Khokhlatchev, A.; Xu, S.; English, J.; Wu, P.; Schaefer, E.; Cobb, M. H. *J. Biol. Chem.* **1997**, *272*, 11057−62.
(34) Forrer, P.; Tamaskovic, R.; Jaussi, R. *J. Biol. Chem.* **1998**, *379*, 1101−11.
(35) Morgan, D. O. *Nature* **1995**, *374*, 131−4.

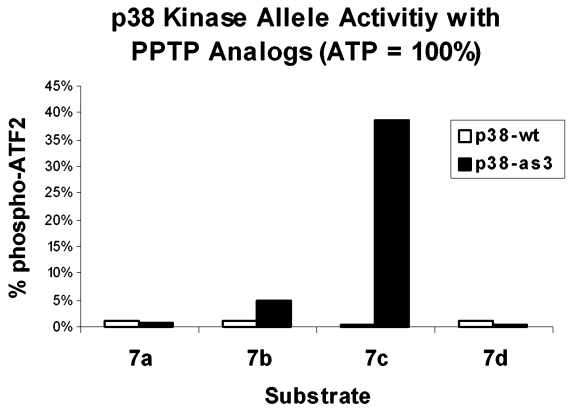

Figure 4. Bar graph showing p38-wt and mutant kinase activity with analogues **7a**−**d**. GST-ATF2 (2 μg) was phosphorylated with p38 in the presence of analogue (100 μM) for 24 h at room temperature. Phosphorylation was measured by ELISA comparing phospho-ATF2 with total ATF2. Data collected for each analogue is reported as a percentage of the phospho-ATF2/total ATF2 that was achieved when ATP was the triphosphate substrate.

Rather than testing the ability of CDK2-as1/E to utilize **7b** and **7c** with a single phosphoacceptor substrate, we asked if these analogues could serve to label a complex cellular lysate when CDK2-as1/E was provided exogenously. This test is identical to the conditions used to label direct CDK2-as1/E substrates and thus is an ideal screen for catalytic efficiency. HeLa cell lysates provided a large pool of protein substrates to be radioactively labeled by the CDK2-as1/E using either [γ-^{32}P]-N^6-(benzyl)-ATP, [γ-^{32}P]-3-benzyl-PPTP, or [γ-^{32}P]-3-phenyl-PPTP (Figure 5). The HeLa cell lysates contain few endogenously active kinases, thus providing a good spectrum of phosphoacceptor substrates for this analysis. Nonradioactive ATP (1mM) and 2 μg of CDK2-as1/E were included and labeling reactions were carried out for 6 min, after which they were separated by SDS PAGE and imaged using a phosphorimager. Both [γ-^{32}P]-N^6-(benzyl)-ATP and [γ-^{32}P]-3-benzyl-PPTP demonstrate high levels of substrate labeling (Figure 5, lanes 1 and 2). Unfortunately, [γ-^{32}P]-3-phenyl-PPTP is a poor substrate for CDK2-as1/E and does not show any significant labeling, suggesting that **7b** may not be a generally useful substrate for mutant protein kinases. These data suggest that [γ-^{32}P]-3-benzyl-PPTP is at least as good a phosphodonor substrate for CDK2-as1/E specific protein substrate labeling as [γ-^{32}P]-N^6-(benzyl)-ATP and shows that they are both capable of competing with high levels of nonradiolabeled ATP.

Kinetics of 3-Benzyl-PPTP-Dependent Phosphorylation. We next investigated the kinetics of peptide phosphorylation by the serine/threonine specific CDK2-as1/E and a tyrosine kinase (v-Src), representing two highly divergent kinase classes. We compared the catalytic efficiency of the wt and as1 mutant alleles with [γ-^{32}P]ATP, [γ-^{32}P]-N^6-(benzyl)-ATP, and [γ-^{32}P]-3-benzyl-PPTP.

In the case of the tyrosine kinase v-Src, the new analogue, [γ-^{32}P]-3-benzyl-PPTP (**7c**) displayed enhanced catalytic efficiency in comparison to [γ-^{32}P]-N^6-(benzyl)-ATP, 3.2×10^6 ($\text{min}^{-1}\,\text{M}^{-1}$) vs 1.0×10^6 ($\text{min}^{-1}\,\text{M}^{-1}$), respectively (Table 1). This improvement in efficiency is largely a result of lowering of the K_M for [γ-^{32}P]-3-benzyl-PPTP, with a small improvement of k_{cat} for this substrate. The improvement in K_M for [γ-^{32}P]-3-benzyl-PPTP is consistent with it being derived from an inhibitor scaffold which itself exhibits nanomolar affinity for the same kinase.[18] Comparison of 3-benzyl-PPTP and engineered v-Src-as1 with the catalytic efficiency of wild-type v-Src with ATP also shows that the substrate design based on the inhibitor scaffold is superior to the naturally occurring enzyme substrate combination.

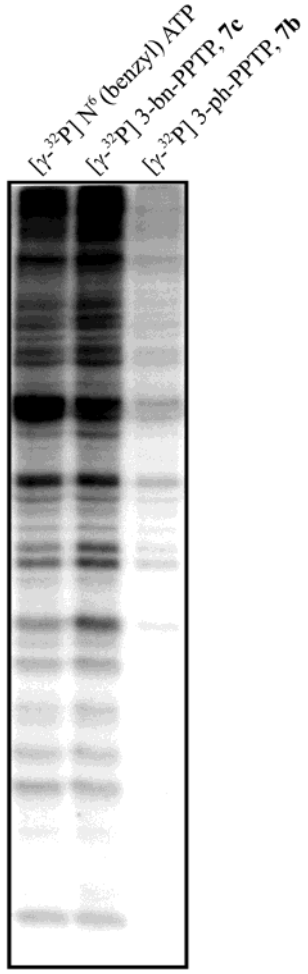

Figure 5. Cell lysate phosphorylation levels are shown, comparing relative activity of [γ-^{32}P]-N^6-(benzyl)-ATP, [γ-^{32}P]-3-benzyl-PPTP, and [γ-^{32}P]-3-phenyl-PPTP by CDK2-as1/E labeling. HeLa cell lysates (4 μL/lane) were incubated with [γ-^{32}P]-N^6-(benzyl)-ATP, [γ-^{32}P]-3-benzyl-PPTP, and [γ-^{32}P]-3-phenyl-PPTP (100 cpm/pmol) for 6 min, separated by 12% SDS−PAGE and exposed to a phosphorimager screen (Molecular Dynamics) for 2 days. Each labeling reaction was run with 2 μg of Cdk2-as1 and 1 mM ATP.

The same general trends were observed in the case of the ser/thr kinase CDK2/E. The K_M was improved by 3-fold for CDK2-as1/E with [γ-^{32}P]-3-benzyl-PPTP compared to CDK2-as1/E with [γ-^{32}P]-N^6-(benzyl)-ATP and by 5-fold as compared to CDK2/E with ATP. The k_{cat} for [γ-^{32}P]-3-benzyl-PPTP with CDK2-as1/E was 40-fold lower than that of [γ-^{32}P]-N^6-(benzyl)-ATP with the same mutant, suggesting that the former is not optimally binding in the CDK2/E ATP binding pocket for efficient phosphate transfer. However, the improved K_M of 3-benzyl-PPTP compared to ATP (>80-fold) implied that this analogue would exhibit efficient labeling of CDK2-as1/E substrates in cell lysates containing high concentrations of ATP. Having established the catalytic efficacy of this analogue, we turned to the question of orthogonality.

3-Phenyl-PPTP (7b) and 3-Benzyl-PPTP (7c) Are Poorly Accepted by Wild-Type Protein Kinases. We performed kinase assays in whole cell lysates to investigate the orthogonal-

Table 1. Kinetic Data for v-Src, v-Src-as1, CDK2/E, and CDK2/E-as1[a]

	ATP			N^6-(benzyl)-ATP			3-benzyl-PPTP		
	K_M, μM	k_{cat}, min^{-1}	k_{cat}/K_M	K_M, μM	k_{cat}, min^{-1}	k_{cat}/K_M	K_M, μM	k_{cat}, min^{-1}	k_{cat}/K_M
v-Src	25	6.7	2.70×10^6	>>1000	na	na	$\gg$1000	na	na
v-Src-as1	150	14	9.30×10^4	2.5	2.6	1.04×10^6	0.32	1	3.20×10^6
CDK2/E WT	32	20	6.30×10^5	>>1000	na	Na	>>1000	na	na
CDK2/E-as1	530	31	5.00×10^4	17	6.4	3.50×10^5	6.4	0.16	2.56×10^4

[a] Kinase reactions were run for 30 min at room temperature. The phosphorylated substrate for Src was the peptide LEEIYGEFKKK (200 μM) and for CDK2/E was histone H1 (500 μg/mL). The triphosphate substrates (100 cpm/pmol) were varied around their respective K_M

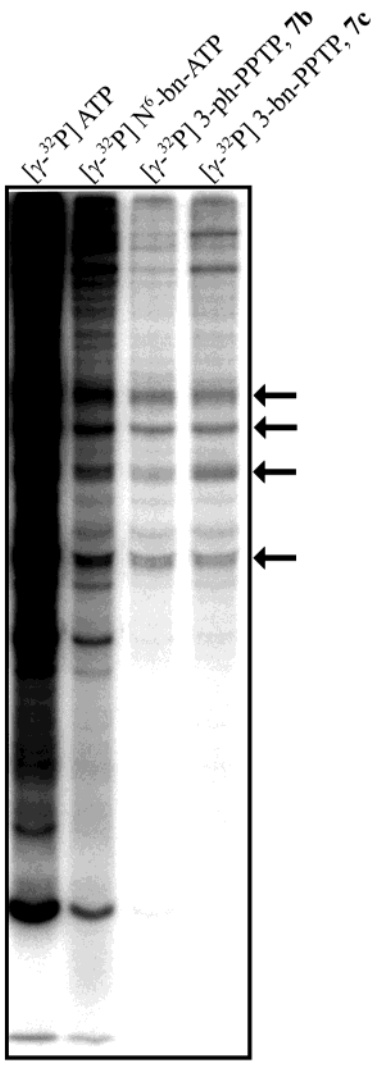

Figure 6. Cell lysate phosphorylation levels showing degree of wild-type kinase utility of ATP or ATP analogues. For each lane 4 $\times$ 10^6 mouse spleenocytes were lysed under hypotonic conditions, incubated 50 s with 200 μM of the given [γ-^{32}P]triphosphate analogue (3.75 cpm/nmol) and then separated on 12% SDS−PAGE and visualized by using a storage phosphor system. For each analogue, the radioactive intensity was quantified for the four protein bands denoted by the arrows.

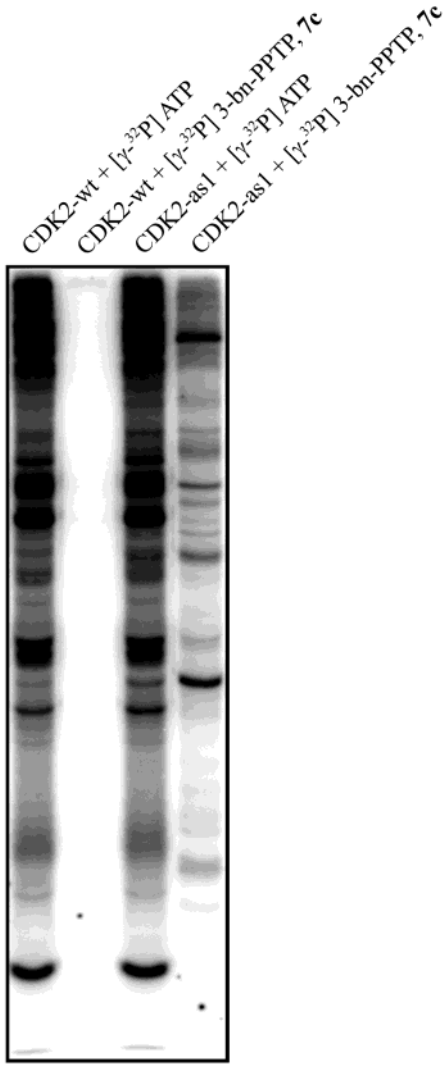

Figure 7. Cell lysate (see Figure 5) phosphorylation levels showing specific CDK2/E substrate labeling by the as1 mutant using [γ^{32}P]-3-benzyl-PPTP and no substrate labeling by the CDK2/E-wt with the analogue. Lane 1 and 3 reactions were run with 200 μM ATP added along with the [γ^{32}P]-ATP (14.5 cpm/nmol). This shows that the kinases and substrates in the cell extracts are viable. Lane 2 and 4 reactions were run with 4 mM cold ATP added along with the indicated analogue (558 cpm/pmol).

ity of two PPTP analogues, **7b** and **7c**. For comparison N^6 (benzyl) ATP and ATP were also included. Hypotonic lysates of murine spleenocytes rich in kinases and their protein substrates were used to assess the ability of a broad range of protein kinases to utilize each analogue as phosphodonor substrates.[36] The [γ-^{32}P] analogues (3.75 cpm/nmol) were incubated with the cell lysates for 50 s and then the proteins were separated by SDS-page and imaged by using a phosphorimager (Figure 6). The presence of many radiolabeled proteins at many molecular weights when [γ-^{32}P]ATP is the phosphodonor shows that this cell lysate is rich with active kinases and their substrates (Figure 6, lane 1). The level of background phosphorylation from wild-type kinases using N^6-(benzyl)-ATP, **7b**, or **7c** is shown in Figure 6, without addition of exogenous ATP. With no added competitor ATP, the sensitivity of this assay is quite high because the radiolabeled analogue is the only

(36) Bolen, J. B.; Rowley, R. B.; Spana, C.; Tsygankov, A. Y. *FASEB J.* **1992**, *6*, 3403−9.

triphosphate substrate present. The analogues that are least accepted by cellular kinases are **7b** and **7c** (Figure 6, lanes 3 and 4). Quantification of the signal with [γ-^{32}P]-N^6-(benzyl)-ATP (Figure 6, lane 2) shows approximately 4 times the level of phosphorylation of the indicated phosphoproteins found in the lane either with **7b** or with **7c**. By this measure the PPTP analogues **7b** and **7c** are 4 times more orthogonal against wild type kinases in a whole cell lysate than the previously reported analogue, [γ-^{32}P]-N^6-(benzyl)-ATP.

Kinase Protein Substrate Labeling in Whole Cell Lysates. We next asked whether the newly designed pyrazolopyrimidine-based orthogonal triphosphate analogue **7c** was capable of efficiently labeling the direct substrates of an analogue specific kinase in whole cell lysates. To specifically radiolabel the direct substrates of CDK2-as1/E in the presence of other active cellular kinases, the highly orthogonal ATP analogue [γ-^{32}P]-3-benzyl-PPTP (**7c)** was used as a specific substrate for the analogue specific CDK2/E mutant kinase (Figure 7).

Several experimental conditions were imposed in order to optimize specific CDK2/E protein substrate labeling. Critical among these was the short 50-s reaction time, which was found to reduce nonspecific labeling noise while maintaining a high degree of specific labeling signal. To mimic the intracellular conditions of high ATP concentration we included nonradio-labeled ATP at a concentration of 4 mM in competition with [γ-^{32}P]-3-benzyl-PPTP. This also further reduced nonspecific radiolabeling background noise. As a test of whether CDK2/E and CDK2-as1/E exhibit the same phosphoprotein substrate specificity and overall catalytic activity, the pattern of protein phosphorylation obtained when either kinase is added to a lysate with [γ-^{32}P]ATP appears identical (Figure 7, lane 1 vs 3).

At least 20 proteins are specifically labeled by CDK2-as1/E in the presence of its designed substrate [γ-^{32}P]-3-benzyl-PPTP (**7c)** which are not observed when wild-type CDK2/E is substituted (Figure 7, lane 4 vs 2). These radiolabeled proteins are currently being analyzed by two-dimensional gel electrophoresis to allow improved separation from comigrating non-labeled cellular proteins, facilitating identification of CDK2/E protein substrates.

Conclusions

Given the large number of protein kinases in the human genome it is a significant challenge to identify an unnatural ATP analogue that is orthogonal to all wild-type kinases and is efficiently accepted by a mutated kinase of interest. A similar challenge arises in efforts to design highly specific protein kinase inhibitors active against only a single kinase in the human genome. Here we have taken lessons from kinase inhibitor design efforts to create a highly specific and orthogonal ATP analogue capable of delivering a radiolabel tag to the direct substrates of the appropriately engineered cell cycle kinase, CDK2/cyclin E. Since the structural features of the mutations which render the three widely divergent kinases studied here (v-Src, p38 MAPK, and CDK2/E) capable of accepting the unnatural phosphodonor, [γ-^{32}P]-3-benzyl-PPTP, are conserved across the entire protein kinase superfamily, we expect this analogue substrate to be generalizable to a majority of protein kinases.

Here we have laid out a systematic approach to the design and implementation of analogue-specific kinase generation coupled with analogue selection and synthesis for that kinase allele. These steps include structural analysis of the kinase of interest or closest related homologue aided by sequence alignment with successful mutants already described in the literature, selection of sensitizing mutations to be made, selection of a small panel of analogues to be tested, biochemical analysis of analogue performance in wt and analogue specific kinase assays, production of radioactive analogues, and finally cell lysate radiolabeling using the analogue specific kinase and [γ-^{32}P] analogue. Kinase mutation selection may require iterative rounds of optimization for activity as well as for specificity toward the analogue and may involve second site mutations (as with p38), which make the kinase more susceptible to the inhibitors or inhibitor based triphosphate analogues. The chemoenzymatic [γ-^{32}P] analogue synthesis is straightforward and robust, accepting four structurally divergent ATP analogues reported here. Finally, conditions for labeling direct substrates from large protein pools have been presented and should be applicable, with only minor adaptation, to almost any kinase or cell type.

Future experiments will focus on the identification of CDK2 and other kinase substrate proteins. Using 2-D electrophoresis and mass spectral analysis of the radioactively labeled proteins, new protein substrates can be identified and candidate substrates evaluated. With the improvements afforded by the improved orthogonality of PPTP analogues, these experiments should be cleaner and allow for the detection of protein substrates too scarce to be detected previously. The search for direct kinase protein substrates can also be extended from cell lysates to whole living cells by using available methods for introduction of nucleotides across cell membranes.[37,38]

Experimental Section

All starting materials were purchased from Sigma/Aldrich and used without further purification. All solvents were purchased from Fisher and, unless otherwise stated, were used without further purification. ^{1}H NMR and ^{13}C NMR spectra were recorded on a Varian 400 spectrometer, at 400 and 100 MHz, respectively, and chemical shifts are reported in parts per million relative to residual protiated solvent. High-resolution electron impact mass spectra were recorded on a MicroMass VG70E spectrometer by Sun Yuequan at the University of California—San Francisco Center for Mass Spectrometry. Reactions were monitored by thin-layer chromatography, using EM Science silica gel 60 F_{254} glass plates (0.25-mm thick). Flash chromatography was conducted with Merck silica gel 60 (230−400 mesh).

2-Phenylacetylmalononitrile (1c): Yield 90%. Sodium hydride (3.60 g, 142 mmol) was suspended in dry THF (25 mL) and the mixture was cooled to 0 °C. Malononitrile (4.70 g, 71.2 mmol) was dissolved in dry THF (25 mL) and added dropwise to the stirring sodium hydride mixture over 20 min. Phenylacetyl chloride (10.0 g, 71.2 mmol) was dissolved in dry THF (25 mL) and added dropwise to the stirring malononitrile solution over 30 min. The reaction was allowed to warm to room temperature and stirred an additional 30 min. Then it was acidified with 1N HCl to pH 2. This mixture was extracted with ethyl acetate (3 × 200 mL) and dried over sodium sulfate. The ethyl acetate was evaporated and the product was purified by flash column chromatography (eluent: EtOAc) to give **1c** as a white solid. R_f = 0.26. ^{1}H NMR (400 MHz, $CDCl_3$) δ 3.88 (s, 2H), 7.33 (vs, 5H), 9.0−9.1 (br s, 1H). ^{13}C NMR (400 MHz, $CDCl_3$) δ 62.50, 112.41, 114.48, 127.26, 127.50, 128.28, 128.46, 128.52, 128.70, 133.51, 187.42. HRMS (EI) M^+ calcd for $C_{11}H_8N_2O$ 184.063 66, found 184.063 74.

(37) Meier, C.; Knispel, T.; De Clercq, E.; Balzarini, J. *J. Med. Chem.* **1999**, *42*, 1604−14.
(38) Dokka, S.; Rojanasakul, Y. *Adv. Drug Delivery Rev.* **2000**, *44*, 35−49.

2-Benzoylmalononitrile (1b): Yield 81%, white solid. ^{1}H NMR (400 MHz, DMSO-d_6) δ 7.45−7.64 (m, 5H), 11.84 (s, 1H). ^{13}C NMR (400 MHz, DMSO-d_6) δ 54.69, 117.12, 118.59, 127.86, 128.32, 128.64, 129.36, 131.45, 135.55, 186.55. HRMS (EI) M^+ calcd for $C_{10}H_6N_2O$ 170.048 01, found 170.048 16.

2-Isobutyrylmalononitrile (1a): Yield 95%, white solid. ^{1}H NMR (400 MHz, DMSO-d_6) δ 0.96 (d, J = 7 Hz, 6H), 2.77 (m, J = 7 Hz, 1H), 6.85 (br s, 1H). ^{13}C NMR (400 MHz, DMSO-d_6) δ 19.30, 34.27, 47.30, 120.18, 121.61, 196.57. HRMS (EI) M^+ calcd for $C_7H_8N_2O$ 136.063 66, found 136.064 00.

2-(1-Methoxy-2-phenylethylidene)malononitrile (2c): Yield 90%. Sodium bicarbonate (45.3 g, 540 mmol) was added over 10 min to a solution of **1c** (12.4 g, 67.4 mmol) in dioxane (120 mL) and water (20 mL). Dimethyl sulfate (59.5 g, 470 mmol) was added and the reaction was heated to reflux with vigorous stirring for 2 h. The reaction was then cooled, diluted with water (100 mL), and extracted with ether (3 × 250 mL). The ether was dried over magnesium sulfate and evaporated under reduced pressure to yield a dark oil. The oil was purified by flash column chromatography (eluent: chloroform/hexanes, 3:2) to give a yellow oil. R_f = 0.25. ^{1}H NMR (400 MHz, $CDCl_3$) δ 3.85 (s, 2H), 3.91 (s, 3H), 7.12−7.30 (m, 5H). ^{13}C NMR (400 MHz, $CDCl_3$) δ 37.71, 59.45, 65.80, 111.43, 113.45, 128.17, 128.29, 129.51, 131.76, 185.96. HRMS (EI) M^+ calcd for $C_{12}H_{10}N_2O$ 198.079 31, found 198.079 27.

2-(Methoxyphenylmethylene)malononitrile (2b): Yield 84%, white solid. ^{1}H NMR (400 MHz, $CDCl_3$) δ 3.90 (s, 3H), 7.46−7.62 (m, 5H). ^{13}C NMR (400 MHz, $CDCl_3$) δ 61.02, 67.77, 111.57, 113.06, 128.06, 128.38, 129.42, 133.03, 184.93. HRMS (EI) M^+ calcd for $C_{11}H_8N_2O$ 184.063 66, found 184.063 92.

2-(1-Methoxy-2-methylpropylidene)malononitrile (2a): Yield 31%, white solid. ^{1}H NMR (400 MHz, $CDCl_3$) δ 1.15 (d, J = 3 Hz, 6H), 3.15 (m, 1H), 4.33 (s, 3H). ^{13}C NMR (400 MHz, $CDCl_3$) δ 19.35, 35.22, 61.12, 61.62, 112.80, 113.40, 191.56. HRMS (EI) M^+ calcd for $C_8H_{10}N_2O$ 150.079 31, found 150.079 27.

2-(1-Methoxy-2-naphthalen-1-ylethylidene)malononitrile (2d): Yield 36%, for 2 steps. Compound **1d** was prepared as for **1a** and was not isolated. Compound **2d** was prepared as for **2c** from the crude **1d** to give a white solid. ^{1}H NMR (400 MHz, $CDCl_3$) δ 3.93 (s, 3H), 4.44 (s, 2H), 7.25 (d, J = 8 Hz, 1H), 7.46 (t, J = 8 Hz, 1H), 7.58 (m, 2H), 7.85 (d, J = 8 Hz, 1H), 7.91 (d, J = 8 Hz, 2H). ^{13}C NMR (400 MHz, $CDCl_3$) δ 34.43, 59.48, 67.82, 111.46, 113.25, 122.24, 125.15, 125.59, 126.49, 127.21, 127.71, 129.09, 129.28, 131.02, 134.02, 186.41; HRMS (EI) M^+ calcd for $C_{16}H_{12}N_2O$ 248.094 96, found 248.094 30.

5-Amino-3-benzyl-1*H*-pyrazole-4-carbonitrile (3c): Yield 52%. Triethylamine (12.4 g, 123 mmol) and hydrazine hydrochloride (4.31 g, 41.0 mmol) were added to a solution of **2c** (8.12 g, 41.0 mmol) in ethanol (200 mL) and refluxed for 15 min. The reaction was evaporated under reduced pressure, re-suspended in water (50 mL), and extracted with ethyl acetate (3 × 200 mL). The extracts were dried over magnesium sulfate and evaporated under reduced pressure. The residue was purified by flash column chromatography (eluent: methanol/chloroform, 1:10) to give a white solid. R_f = 0.23. ^{1}H NMR (400 MHz, DMSO-d_6) δ 3.68 (s, 2H), 7.26−7.37 (m, 5H). ^{13}C NMR (400 MHz, DMSO-d_6) δ 52.80, 116.11, 119.07, 126.64, 128.14, 128.5, 128.72, 136.61, 166.29. HRMS (EI) M^+ calcd for $C_{11}H_{10}N_4$ 198.090 55, found 198.090 01.

5-Amino-3-phenyl-1*H*-pyrazole-4-carbonitrile (3b): Yield 75%, white solid. ^{1}H NMR (400 MHz, DMSO-d_6) δ 6.48 (s, 2H), 7.41−7.47 (m, 3H), 7.82 (d, J = 7 Hz, 2H), 12.16 (s, 1H). ^{13}C NMR (400 MHz, DMSO-d_6) δ 69.56, 116.28, 125.65, 128.52, 128.69, 132.14, 150.04, 154.67. HRMS (EI) M^+ calcd for $C_{10}H_8N_4$ 184.074 90, found 184.074 96.

5-Amino-3-isopropyl-1*H*-pyrazole-4-carbonitrile (3a): Yield 72%, white solid. ^{1}H NMR (400 MHz, DMSO-d_6) δ 1.33 (d, J = 7 Hz, 6H), 3.05 (m, 1H), 5.72 (br s, 2H). ^{13}C NMR (400 MHz, DMSO-d_6) δ 21.09, 26.83, 76.54, 114.29, 156.35, 156.62. HRMS (EI) M^+ calcd for $C_7H_{10}N_4$ 150.090 55, found 150.090 04.

5-Amino-3-naphthalen-1-ylmethyl-1*H*-pyrazole-4-carbonitrile (3d): Yield 84%, white solid. ^{1}H NMR (400 MHz, DMSO-d_6) δ 4.26 (s, 2H), 6.29 (s, 2H), 7.38−7.52 (m, 4H), 7.82 (d, J = 7 Hz, 1H), 7.93 (d, J = 6 Hz, 1H), 8.19 (s, 1H), 11.70 (s, 1H). ^{13}C NMR (400 MHz, DMSO-d_6) δ 31.19, 71.75, 115.44, 124.12, 125.49, 125.64, 125.94, 126.90, 127.08, 128.44, 131.53, 133.40, 134.22, 151.76, 153.57. HRMS (EI) M^+ calcd for $C_{15}H_{12}N_4$ 248.106 20, found 248.106 47.

3-Benzyl-1*H*-pyrazolo[3,4-*d*]pyrimidin-4-ylamine (4c): Yield 72%. Compound **3c** (6.74 g, 34.0 mmol) was suspended in formamide (100 mL) and heated to 180 °C overnight. The reaction was cooled to room temperature and poured into water (400 mL), and the precipitate that formed was collected. This precipitate was redissolved in a minimum of hot ethanol, decolorized with charcoal, and filtered through Celite. SiO_2 (30 g) was added to the filtrate and the solvent was evaporated under reduced pressure. This dried SiO_2 was then poured onto a column of SiO_2 and purified by flash column chromatography (eluent: methanol/chloroform 1:20) to give a white solid. R_f = 0.19. ^{1}H NMR (400 MHz, DMSO-d_6) δ 4.35 (s, 2H), 7.05 (br s, 2H), 7.18−7.30 (m, 5H), 8.12 (s, 1H), 13.14 (s, 1H). ^{13}C NMR (400 MHz, DMSO-d_6) δ 33.46, 97.92, 126.15, 128.37, 128.53, 139.23, 143.82, 155.67, 155.95, 157.96. HRMS (EI) M^+ calcd for $C_{12}H_{11}N_5$ 225.101 45, found 225.101 56.

3-Phenyl-1*H*-pyrazolo[3,4-*d*]pyrimidin-4-ylamine (4b): Yield 72%, white solid. ^{1}H NMR (400 MHz, DMSO-d_6) δ 6.8 (br s, 2H), 7.49−7.70 (m, 5H), 8.25 (s, 1H), 13.61 (s, 1H). ^{13}C NMR (400 MHz, DMSO-d_6) δ 96.96, 128.23, 128.49, 129.09, 155.79, 156.06, 158.04. HRMS (EI) M^+ calcd for $C_{11}H_9N_5$ 211.085 80, found 211.085 36.

3-Isopropyl-1*H*-pyrazolo[3,4-*d*]pyrimidin-4-ylamine (4a): Yield 70%, white solid. ^{1}H NMR (400 MHz, DMSO-d_6) δ 1.25 (m, 6H), 3.48 (m, 1H), 7.43 (br s, 1H), 8.08 (s, 1H), 12.91 (s, 1H). ^{13}C NMR (400 MHz, DMSO-d_6) δ 22.09, 27.06, 97.11, 150.42, 155.47, 157.96, 162.96. HRMS (EI) M^+ calcd for $C_8H_{11}N_5$ 177.101 45, found 177.102 13.

3-Naphthalen-1-ylmethyl-1*H*-pyrazolo[3,4-*d*]pyrimidin-4-ylamine (4d): Yield 60%, white solid. ^{1}H NMR (400 MHz, DMSO-d_6) δ 4.80 (s, 2H), 7.138 (broad s, 2H), 7.25 (d, J = 7 Hz, 1H), 7.40 (t, J = 8 Hz, 1H), 7.51 (t, J = 5 Hz, 1H), 7.53−7.54 (m, 1H), 7.81 (d, J = 8 Hz, 1H), 7.92−7.94 (m, 1H), 8.14−8.19 (m, 2H). ^{13}C NMR (400 MHz, DMSO-d_6) δ 31.46, 98.36, 124.42, 125.52, 125.62, 125.85, 126.17, 126.91, 128.35, 131.64, 133.40, 135.21, 143.41, 155.67, 158.05. HRMS (EI) M^+ calcd for $C_{16}H_{13}N_5$ 275.117 10, found 275.116 95.

1-((2*S*,3*R*,4*S*,5*R*)-3,4-Dibenzoyl-5-benzoylmethyltetrahydrofuran-2-yl)-3-benzyl-1*H*-pyrazolo[3,4-*d*]pyrimidin-4-ylamine (5c): Yield 80%. Compound **4c** (0.50 g, 2.2 mmol) and β-*d*-ribofuranose 1-acetate-2,3,5-tribenzoate (1.1 g, 2.2 mmol) were placed in a flame-dried flask with a stir bar under argon. Dry acetonitrile (22 mL, distilled over CaH_2) was added by syringe and the mixture was stirred for 10 min. $SnCl_4$ (1.5 g, 5.5 mmol) was added by syringe to the reaction and a homogeneous mixture was obtained after about 2 min. After 5 h the reaction was quenched by addition of saturated sodium bicarbonate (50 mL) and the mixture was extracted with ethyl acetate (3 × 50 mL). The organic layer was dried over Na_2SO_4 and then purified further by flash column chromatography (eluent: methanol/chloroform, 1:20) to give a white solid. R_f = 0.28. ^{1}H NMR (400 MHz, $CDCl_3$) δ 4.24 (m, 2H), 4.68 (m, 1H), 4.84−4.87 (m, 2H), 5.16 (br s, 2H), 6.38 (t, J = 6 Hz, 1H), 6.53 (t, J = 4 Hz, 1H), 6.89 (d, J = 3 Hz), 7.22−7.61 (m, 14H), 8.00 (d, J = 8 Hz, 2H), 8.03 (d, J = 8 Hz, 2H), 8.15 (d, J = 8 Hz, 2H), 8.31 (s, 1H). ^{13}C NMR (400 MHz, $CDCl_3$) δ 35.17, 64.11, 72.18, 74.38, 80.05, 86.59, 100.00, 127.57, 128.27, 128.41, 128.44, 128.51, 128.88, 128.93, 129.43, 129.71, 129.78, 129.85, 129.87, 133.03, 133.47, 133.50, 137.09, 145.79, 156.14, 156.32, 157.44, 165.14, 165.34, 166.20. HRMS (EI) M^+ calcd for $C_{38}H_{31}N_5O_7$ 669.222 35, found 669.228 93.

1-((2*S*,3*R*,4*S*,5*R*)-3,4-Dibenzoyl-5-benzoylmethyltetrahydrofuran-2-yl)-3-phenyl-1*H*-pyrazolo[3,4-*d*]pyrimidin-4-ylamine (5b): Yield 70%, white solid. ^{1}H NMR (400 MHz, $CDCl_3$) δ 4.55−4.78 (m, 3H), 5.56 (br s, 2H), 6.24 (t, J = 6 Hz, 1H), 6.42 (t, J = 6 Hz, 1H), 6.84 (d, J = 3 Hz, 1H), 7.11−7.48 (m, 12H), 7.59 (m, 2H), 7.86 (d, J = 8 Hz,

2H), 7.90 (d, $J = 7$ Hz, 2H), 7.96 (d, $J = 7$ Hz, 2H), 8.31 (s, 1H). ^{13}C NMR (400 MHz, $CDCl_3$) δ 64.08, 72.03, 74.42, 80.05, 86.80, 99.18, 128.25, 128.42, 128.45, 128.57, 128.89, 128.93, 129.39, 129.56, 129.78, 129.82, 129.87, 132.69, 132.96, 133.47, 133.56, 146.45, 155.89, 156.40, 157.77, 165.13, 165.32, 166.26. HRMS (EI) M^+ calcd for $C_{37}H_{29}N_5O_7$ 655.206 70, found 655.206 72.

1-((2*S*,3*R*,4*S*,5*R*)-3,4-Dibenzoyl-5-benzoylmethyltetrahydrofuran-2-yl)-3-isopropyl-1*H*-pyrazolo[3,4-*d*]pyrimidin-4-ylamine (5a): Yield 77%, white solid. ^{1}H NMR (400 MHz, $CDCl_3$) δ 1.38 (d, $J = 2$ Hz, 3H), 1.40 (d, $J = 2$ Hz, 3H), 3.16 (m, 1H), 4.62 (m, 1H), 4.72−4.83 (m, 2H), 5.78 (br s, 2H), 6.32−6.39 (m, 2H), 6.80 (d, 1H), 7.31−7.56 (m, 14H), 7.92 (d, $J = 7$ Hz, 2H), 7.98 (d, $J = 8$ Hz, 2H), 8.03 (d, $J = 8$ Hz, 2H), 8.32 (s, 1H). ^{13}C NMR (400 MHz, $CDCl_3$) δ 21.35, 21.63, 29.17, 64.62, 72.34, 74.55, 19.72, 86.58, 99.35, 128.28, 128.37, 128.43, 128.90, 128.92, 129.60, 129.74, 129.77, 129.83, 133.03, 133.42, 133.52, 152.24, 155.81, 156.10, 157.68, 165.16, 165.31, 166.19. HRMS (EI) $(M + H)^+$ calcd for $C_{34}H_{32}N_5O_7$ 622.230 17, found 622.230 33.

1-((2*S*,3*R*,4*S*,5*R*)-3,4-Dibenzoyl-5-benzoylmethyltetrahydrofuran-2-yl)-3-naphthalen-1-ylmethyl-1*H*-pyrazolo[3,4-*d*]pyrimidin-4-ylamine (5d): Yield 52%, white solid. ^{1}H NMR (400 MHz, $CDCl_3$) δ 4.57−4.71 (m, 3H), 4.88 (m, 2H), 5.03 (br s, 2H), 6.39 (t, $J = 5$ Hz, 1H), 6.59 (t, $J = 4$ Hz, 1H), 6.91 (d, $J = 4$ Hz, 1H), 7.25−7.61 (m, 15H), 7.84 (d, $J = 8$ Hz, 1H), 7.91 (d, $J = 8$ Hz, 1H), 8.00−8.05 (m, 3H), 8.15 (m, 2H), 8.30 (s, 1H). ^{13}C NMR (400 MHz, $CDCl_3$) δ 32.89, 64.17, 72.35, 74.35, 80.20, 56.51, 100.45, 123.52, 125.54, 126.18, 126.36, 126.90, 128.26, 128.42, 128.46, 128.54, 128.90, 129.02, 129.81, 129.88, 129.90, 131.81, 132.96, 133.00, 133.47, 133.54, 134.07, 145.57, 156.34, 157.43, 165.14, 165.37, 166.20. HRMS (EI) M^+ calcd for $C_{42}H_{33}N_5O_7$ 719.238 00, found 719.237 57.

(2*S*,3*R*,4*S*,5*R*)-2-(4-Amino-3-benzylpyrazolo[3,4-*d*]pyrimidin-1-yl)-5-hydroxymethyltetrahydrofuran-3,4-diol (6c): Yield 80%. Compound **5c** (1.07 g, 1.60 mmol) was dissolved in 7 N ammonia in methanol (40 mL). The flask was sealed with a septum and stirred at room temperature for 36 h after which the solvent was evaporated and the product was purified flash column chromatography (eluent: methanol/chloroform, 1:10) to give a white solid. $R_f = 0.24$. ^{1}H NMR (400 MHz, DMSO-d_6) δ 3.44 (m, 1H), 3.56 (m, 1H), 3.89 (d, $J = 5$ Hz, 1H), 4.22 (d, $J = 5$ Hz, 1H), 4.36 (s, 2H), 4.59 (m, 1H), 4.85 (m, 1H), 5.09 (d, $J = 6$ Hz, 1H), 5.34 (d, $J = 6$ Hz, 1H), 6.07 (d, $J = 4$ Hz), 7.19−7.29 (m, 5H), 8.17 (s, 1H). ^{13}C NMR (400 MHz, DMSO-d_6) δ 33.25, 62.45, 70.89, 73.05, 85.01, 88.39, 98.86, 126.29, 128.40, 128.51, 138.55, 144.49, 155.207, 155.92, 158.02. HRMS (EI) $(M + H)^+$ calcd for $C_{17}H_{20}N_5O_4$ 358.151 53, found 358.151 89.

(2*S*,3*R*,4*S*,5*R*)-2-(4-Amino-3-phenylpyrazolo[3,4-*d*]pyrimidin-1-yl)-5-hydroxymethyltetrahydrofuran-3,4-diol (6b): Yield 81%, white solid. ^{1}H NMR (400 MHz, DMSO-d_6) δ 3.48 (m, 1H), 3.61 (m, 1H), 3.95 (m, 1H), 4.28 (m, 1H), 4.85 (t, $J = 6$ Hz, 1H), 5.15 (d, $J = 6$ Hz, 1H), 5.42 (d, $J = 6$ Hz, 1H), 6.21 (d, $J = 4$ Hz, 1H), 7.50−7.60 (m, 3H), 7.69 (d, $J = 7$ Hz, 2H), 8.29 (s, 1H). ^{13}C NMR (400 MHz, DMSO-d_6) δ 62.36, 70.90, 73.23, 85.19, 88.43, 97.83, 128.23, 128.94, 129.20, 132.60, 144.85, 155.33, 156.04, 158.17. HRMS (EI) $(M + H)^+$ calcd for $C_{16}H_{18}N_5O_4$ 344.135 88, found 344.135 42.

(2*S*,3*R*,4*S*,5*R*)-2-(4-Amino-3-isopropylpyrazolo[3,4-*d*]pyrimidin-1-yl)-5-hydroxymethyltetrahydrofuran-3,4-diol (6a): Yield 83%, white solid. ^{1}H NMR (400 MHz, DMSO-d_6) δ 1.27 (d, $J = 7$ Hz, 6H), 3.33−3.62 (m, 3H), 3.91 (m, 1H), 4.26 (m, 1H), 4.57 (m, 1H), 4.86 (m, 1H), 5.08 (d, $J = 6$ Hz, 1H), 5.32 (d, $J = 6$ Hz, 1H), 6.06 (d, $J = 4$ Hz, 1H), 7.31 (br s, 2H), 8.16 (s, 1H). ^{13}C NMR (400 MHz, DMSO-d_6) δ 22.42, 22.50, 27.67, 63.22, 71.74, 73.96, 85.81, 89.30, 98.79, 151.83, 155.68, 156.41, 158.71. HRMS (EI) $(M + H)^+$ calcd for $C_{13}H_{20}N_5O_4$ 310.151 53, found 310.150 83.

(2*S*,3*R*,4*S*,5*R*)-2-(4-Amino-3-naphthalen-1-ylmethylpyrazolo[3,4-*d*]pyrimidin-1-yl)-5-hydroxymethyltetrahydrofuran-3,4-diol (6d): Yield 64%, white solid. ^{1}H NMR (400 MHz, DMSO-d_6) δ 3.25−3.31 (m, 1H), 3.44−3.48 (m, 1H), 3.85 (m, 1H), 4.11 (m, 1H), 4.50 (m, 1H), 4.75 (m, 1H), 4.81 (s, 2H), 5.03 (d, $J = 6$ Hz, 1H), 5.30 (d, $J = 6$ Hz, 1H), 6.04 (d, $J = 4$ Hz, 1H), 7.24 (d, $J = 7$ Hz, 1H), 7.41 (t, $J = 8$ Hz, 1H), 7.53 (m, 2H), 7.82 (d, $J = 8$ Hz, 1H), 7.93 (m, 1H), 8.19 (s, 1H), 8.25 (d, $J = 8$ Hz, 1H). ^{13}C NMR (400 MHz, DMSO-d_6) δ 31.15, 62.51, 70.95, 73.08, 85.03, 88.47, 99.38, 124.39, 125.49, 125.72, 125.90, 127.07, 128.36, 131.60, 133.38, 134.65, 144.02, 155.10, 155.92, 158.11. HRMS (EI) M^+ calcd for $C_{21}H_{21}N_5O_4$ 407.159 35, found 407.159 25.

(2*S*,3*R*,4*S*,5*R*)-2-(4-Amino-3-benzylpyrazolo[3,4-*d*]pyrimidin-1-yl)-5-hydroxymethyltetrahydrofuran-3,4-diol-5′-triphosphate (3-Benzyl-PPTP, 7c): Isolated yield 2%. The nucleoside **6c** (71 mg, 0.20 mmol) was suspended in trimethyl phosphate (0.50 mL) under argon at 0 °C. Phosphorus oxychloride (98 mg, 0.64 mmol) was added by syringe to the stirring mixture. After 5 min a homogeneous mixture was obtained. After 40 min, dry *tert*-butylpyrophosphoric acid (see below) was dissolved in DMF (2 mL) and poured into the reaction. After 1 min this mixture was neutralized with triethylammonium bicarbonate (1 N, pH 7.5, 2 mL). The volatile materials were then evaporated under reduced pressure at 37 °C. The resulting white solid was dissolved in water (2 mL) and purified by HPLC (PerSeptive Biosystems Poros HQ/M strong anion exchange column. Gradient: water ? 30% TEAB {1 N, pH 7.5} over 20 min; flow rate, 15 mL/min, retention time for **7c** was 8.8 min). The fractions containing 3-benzyl-PPTP were collected, evaporated under reduced pressure, and dissolved in water, and then the pH was adjusted to 7.5 with 0.1 N hydrochloric acid. ESI-MS M^- calcd for $C_{17}H_{18}N_5O_{13}P_3$ 596, found 596. Compound **7c** was found to be 99% pure by HPLC (Poros HQ/H anion exchange column. Gradient: 0% → 30% TEAB {1 N, pH 7.5} over 12 min; flow rate, 3 mL/min; retention time for 7c was 8.9 min).

The pyrophosphoric acid mixture was prepared the day before use by combining pyrophosphoric acid (178 mg, 1.0 mmol) in water (2 mL) and ethanol (2 mL) with tributylamine (370 mg, 2.0 mmol) and evaporating the solvent; first by rotary evaporator and then over phosphorus pentoxide under vacuum for 18 h.

(2*S*,3*R*,4*S*,5*R*)-2-(4-Amino-3-phenylpyrazolo[3,4-*d*]pyrimidin-1-yl)-5-hydroxymethyltetrahydrofuran-3,4-diol-5′-triphosphate (3-Phenyl-PPTP, 7b): Isolated yield 3%. HPLC retention time 9.0 min. ESI-MS M^- calcd for $C_{16}H_{19}N_5O_{13}P_3$ 582, found 582.

(2*S*,3*R*,4*S*,5*R*)-2-(4-Amino-3-isopropylpyrazolo[3,4-*d*]pyrimidin-1-yl)-5-hydroxymethyltetrahydrofuran-3,4-diol-5′-triphosphate (3-Isopropyl-PPTP, 7a): Isolated yield 5%. HPLC retention time 8.8 min. ESI-MS M^- calcd for $C_{13}H_{21}N_5O_{13}P_3$ 548, found 548.

(2*S*,3*R*,4*S*,5*R*)-2-(4-Amino-3-naphthalen-1-ylmethylpyrazolo-[3,4-*d*]pyrimidin-1-yl)-5-hydroxymethyltetrahydrofuran-3,4-diol-5′-triphosphate (3-(1-NM)-PPTP, 7d): Isolated yield 1%. HPLC retention time 14.1 min. ESI-MS M^- calcd for $C_{21}H_{23}N_5O_{13}P_3$ 646, found 646.

(2*S*,3*R*,4*S*,5*R*)-2-(4-Amino-3-benzylpyrazolo[3,4-*d*]pyrimidin-1-yl)-5-hydroxymethyltetrahydrofuran-3,4-diol-5′-diphosphate (3-Benzyl-PPDP, 7e): Method A: Yield 2%. Nucleoside **6c** (71 mg, 0.2 mmol) was suspended in trimethyl phosphate (0.5 mL) under argon at 0 °C. Phosphorus oxychloride (98 mg, 0.64 mmol) was added to the stirring mixture by syringe. After 5 min, a homogeneous mixture was obtained. After 40 min, the reaction was quenched with triethylammonium bicarbonate (1 N, pH 7.5, 2 mL) and evaporated to dryness under reduced pressure at 40 °C. The residue was then dissolved in water and 3-benzyl-PP-monophosphate was purified by HPLC (PerSeptive Biosystems Poros HQ/M strong anion exchange column. Gradient: water → 30% TEAB {1 N, pH 7.5} over 20 min; flow rate, 15 mL/min; retention time for 3-benzyl-PP-monophosphate was 4.1 min). The fractions containing 3-benzyl-PP-monophosphate were collected and dried under reduced pressure in preparation for the next reaction. 3-Benzyl-PP-5″-monophosphate (157 mg, 360 μmol) was dissolved in DMF (6 mL) along with carbonyldiimidazole (526 mg, 3.24 mmol) and stirred overnight under argon at room temperature. The excess carbonyldiimidazole was then destroyed by addition of methanol (233 μL, 5.76 mmol), followed by phosphoric acid (392 mg,

4.0 mmol, dried over P_2O_5) dissolved in dry DMF (2 mL). The mixture was then stirred under argon for 3 h at room temperature, after which it was quenched with TEAB (1 N, pH = 7.5, 2 mL), dried, and purified by HPLC (PerSeptive Biosystems Poros HQ/M strong anion exchange column. Gradient: water → 30% TEAB {1 N, pH 7.5} over 20 min; flow rate, 15 mL/min; retention time for **7e** was 7.0 min). Method B: Yield 70%. Nucleotide **7c** (800 nmol) was degraded in water (1 mL) with hexokinase (1 mg, 30 units) and glucose (5 mM) for 1 min at room temperature. The diphosphate was then isolated by HPLC as for method A.

Both methods produced **7e** found to be 99% pure by analytical HPLC (Poros HQ/H anion exchange column. Gradient: water → 30% TEAB (1 N, pH 7.5) over 12 min; flow rate, 3 mL/min; retention time for **7e** was 6.6 min). Synthesis of the diphosphate was also confirmed by positive enzymatic reaction with NDPK to make the [γ-^{32}P]-3-benzyl-PPTP (see procedure above).

(2*S*,3*R*,4*S*,5*R*)-2-(4-Amino-3-phenylpyrazolo[3,4-*d*]pyrimidin-1-yl)-5-hydroxymethyltetrahydrofuran-3,4-diol-5′-diphosphate (3-Phenyl-PPDP, 7f): Yield 2%. Prepared as for 3-benzyl-PPDP. HPLC retention time 6.3 min.

Enzymatic Synthesis of [γ-^{32}P] Triphosphate Analogues. ADP analogues were converted to [γ-^{32}P] triphosphates by means of phosphate transfer reactions utilizing purified recombinant nucleoside diphosphate kinase (NDPK). The *Saccharomyces cerevisiae* gene encoding NDPK (Ynk1) was PCR amplified from genomic DNA and cloned into the bacterial expression vector pET19b (Novagen), which incorporates an amino-terminal 10X-His tag. The construct was expressed in BL21 *Escherichia coli* by induction with 0.4 mM IPTG for 4 h at 30 °C. Cells were lysed by sonication following pretreatment with lysozyme. NDPK was purified by metal affinity chromatography using IDA Sepharose charged with Co^{2+}. NDPK bound to the column was found to resist elution by 300 mM imidazole; this allowed for extensive washing before elution of the protein using 100 mM EDTA. The eluate was dialyzed against storage buffer (150 mM NaCl, 20 mM HEPES pH 7.4, 10% glycerol) and stored at −80 °C. The protein obtained in this manner was found to be essentially pure as judged by SDS−PAGE.

To effect the [γ-^{32}P] transfer, Co^{2+} charged Sepharose (200 μL, 1:1 slurry of water/Sepharose) was placed in a disposable column and washed (3×, 1 mL) with elution buffer (5 mM $MgCl_2$ in HBS). The Sepharose was then charged with NDPK (8.6 nmol) and washed again with elution buffer (3×, 1 mL). The immobilized NDPK was then charged with ^{32}P by adding [γ-^{32}P]ATP (2 mCi, ICN end labeling grade; 7000 Ci/mmol = 285 pmol) in elution buffer (400 μL). The column was then washed again with elution buffer (3×, 1 mL). Finally, the analogue diphosphate (2.7 nmol) diluted in elution buffer (50 μL) was added to the column and three fractions were collected (200 μL). These last three washes containing the [γ-^{32}P] analogue were used directly in either kinase activity or cell lysate labeling experiments.

Src Kinase Production. v-Src (XD4) wt and as-1 (T338G) were both produced as described by Shah, et al.[11]

p38 MAPK Production. Active wild type and mutant p38 proteins were expressed in BL21(DE3) *E. coli* as 6-His constructs by using an expression system developed by M. H. Cobb and co-workers.[33] The two plasmids for this system were a generous gift from their lab: (i) pT7-5 plasmid containing the genes encoding p38, MEK4, and ampicillin resistance and (ii) pBB131 plasmid containing the genes encoding a constitutively active form of MEKK-C and kanamycin resistance. The two plasmids were co-transformed and selected for with appropriate antibiotics. A single colony was then cultured in 250 mL of LB to log phase growth and induced with 0.25 mM IPTG for 12 h. The protein was then purified by using a B-PER 6His spin purification kit (Pierce).

Analogue-specific mutant **3** refers to the mutation made at T106 to glycine. This analogue sensitive allele also contains A157L and L167A mutations to sensitize P38 to the PP1-based inhibitors and the PPTP's.

Preparation of Cyclin−CDK Complexes. Sf9 cells were infected with baculovirus encoding human CDK2-wt, as1, or cyclin E. CDKs were tagged at the carboxy terminus with a hemagglutinin epitope tag, and the cyclin contained an amino-terminal six-His tag. Cyclin E/CDK complexes were assembled by mixing the appropriate Sf9 extracts. Activation of cyclin-CDK complexes was accomplished by the addition of 1 mM ATP, 10 mM $MgCl_2$, and a small amount of Sf9 extract containing baculovirus-expressed human CDK-activating kinase. Kinase complexes were purified by iminodiacetic acid (IDA)-Co^{2+} affinity chromatography and stored at −80 °C in storage buffer (150 mM NaCl, 20 mM HEPES pH 7.4, 10% glycerol).

p38 Activity with NTPs. Kinase reactions were performed with 100 μM NTP, 2 μg GST-ATF-2, and 10 ng p38 in 30 μL of kinase buffer (50 mM Tris pH 7.4, 20 mM MgCl, 100 μM DTT, 100 μg/mL BSA, 1 mM Pefabloc). The reactions were run 24 h at room temperature and then the extent of ATF2 phosphorylation was measured by using an ELISA-based assay in anti-GST strip plates (Pierce). Aliquots (3 μL) of each analogue/kinase reaction were added to duplicate plates and diluted with TBST (197 μL, 0.05% Tween 20, 1× TBS). Both strip plates were incubated for 1 h at room temperature and then washed with TBST (4×, 100 μL). The first plate was then treated with a solution of anti-Phospho-ATF-2 (Thr71) (100 μL, dil 1:500, Cell Signaling Technology-(CST)). The duplicate was treated with an anti-ATF-2 antibody (100 μL, dil 1:1000, CST). Each was incubated for 1 h at room temperature, washed with TBST (4×, 100 μL), and then the secondary antibody was added (100 μL, dil 1:10,000, GAR−IgG-HRP, CST). The plates were incubated 45 min at room temperature and washed with TBST again (4×, 100 μL). Finally TMB substrate (Pierce) was added (100 μL) and incubated for 5 min. The development was stopped by the addition of H_2SO_4 (2 N, 100 μL) and an OD (450 nm) was taken.

Src and CDK Kinase Kinetic Data. The Src kinase reaction buffer was 50 mM Tris pH 8.0, 10 mM $MgCl_2$, 100 μg /mL BSA, and 100 mM NaCl. The CDK2 reaction buffer was 25 mM HEPES pH 7.5, 10 mM $MgCl_2$, 100 μg /mL BSA, and 150 mM NaCl. The kinase substrates used were LEEIYGEFKKK for Src and histone H1 for CDK2 and analogue concentrations used were varied around the K_M of the given kinase, wild type or mutant, for the given analogue. Analogue activity was 100 cpm/pmol. The reactions were quenched after 30 min at room temperature by spotting 27 μL of each 30 μL total reaction mixture onto phosphocellulose (Whatman p81) paper disks. The disks were washed for 5 min in 10% acetic acid, followed by three, 5-min washes with 0.5% phosphoric acid, and a final 1-min wash with acetone. Liquid scintillation counting was used to measure the extent of phosphotransfer.

Cell Lysates. HeLa cell lysates used for the labeling experiment shown in Figure 5 were prepared from a 3-mL pellet of HeLa cells purchased from the National Cell Culture Center (NCCC). The frozen pellet was treated with 20 mL of 25 mM HEPES (pH 7.5), 150 mM KCl, 2 mM EGTA, 1% NP-40, 1% deoxycholate, 1 mM Na_3VO_4, 10 mM NaF, 1 mM PMSF, and 2 tablets of complete mini protease inhibitor cocktail (Roche). They were incubated (30 min) and sonicated and insolubles were removed by centrifugation. Glycerol was added to 10% and 200-μL aliquots were stored at −20 °C.

The mouse spleenocyte cell lysates used for the labeling experiments (Figures 6 and 7) were prepared immediately prior to each experiment. A spleenectomy was performed on a C57B/6 mouse. Spleenocytes were isolated by crushing the spleen in complete RPMI, passage through a nylon mesh, and then centrifugation for 10 min at 1200 rpm (300*g*). The resulting pellet was resuspended in ACK buffer (0.15 M NH_4Cl, 10 mM $KHCO_3$, 0.1 mM EDTA, pH 7.3) to lyse the red blood cells. The remaining spleenocytes were then pelletted by centrifugation and lysed by resuspension in a hypotonic buffer (120 μL, 1 mM HEPES, pH 7.4) at 0 °C for 30 min. Bulk debris was removed by centrifugation at 14 000 rpm in a microcentrifuge for 20 min at room temperature. The supernatant was then brought to 1 mM NaF, 100 μM Na_3VO_4,

and 1 μM in Okadaic Acid and stored at 0 °C for at least 20 min more before starting the labeling experiment.

Protein Labeling of Cell Lysates with CDK2 Alleles and [γ-32P] Analogues. The lysates prepared above were mixed with CDK2 kinase buffer (see below) and either water or CDK2 wild type or mutant. To start the reactions either [γ-^{32}P]ATP, [γ-^{32}P]-N^6-(benzyl)-ATP, [γ-^{32}P]-3-phenyl-PPTP, or [γ-^{32}P]-3-benzyl-PPTP (activity and amounts are listed in the caption for each figure) was added to bring each reaction to 30 μL. The reactions were incubated for 50 s at room temperature and then terminated by addition of 10 μL gel loading buffer (62.5 mM Tris pH 6.8, 2.5% SDS, 10% glycerol, 2.5 mg/mL DTT, 2.5% BME final concentration) and heating to 95 °C for 5 min. The labeled proteins were separated by 12% SDS-page. Autoradiography was performed by using a storage phosphor system (screen-Molecular Dynamics, imager-Storm 850).

Acknowledgment. This work was supported by a grant for the National Institute of Health (1R011CA70331-01) to K.M.S. Mass spectra were provided by the Center for Mass Spectrometry at the University of California—San Francisco, supported by the NIH Division of Research Resources. HeLa cell lysates were provided by the National Cell Culture Center. We thank Anthony Bishop for his work with p38 analogue specific mutants and Jeff Ubersax for his generous donation of protein. We thank members of the Shokat lab, and especially Peter Alaimo, Zachary Knight, Scott Ulrich and Chao Zhang, for helpful discussions and advice.

JA0264798